International Journal of Heat and Technology
Vol. 40, No. 5, October, 2022, pp. 1141-1149
Journal homepage: http://iieta.org/journals/ijht

Numerical Simulation of Influencing Factors to the Thermal Insulation Performance of Cold Chain Shipping Containers and Analysis of Internal Flow Field

Shouhui He[1*], Yan Wang[2], Hongda Liu[3]

[1] School of Logistics, Linyi University, Linyi 276000, China
[2] Linyi Zhixing Traffic Planning & Design Co., LTD, Linyi 276000, China
[3] People's Political Consultative Conference of Fei Country, Linyi 276000, China

Corresponding Author Email: supremehe@163.com

https://doi.org/10.18280/ijht.400504

Received: 15 June 2022
Accepted: 2 September 2022

Keywords:
cold chain shipping containers, thermal insulation performance, numerical simulation, internal flow field analysis

ABSTRACT

Cold chain transportation can prolong the shelf lives of products and reduce losses, so based on the practical applications, it is necessary to numerically simulate the flow field and thermal insulation performance of cold chain shipping containers. Existing studies have achieved optimization by changing the thermal performance and thermal insulation mechanisms of the thermal insulation materials of the containers, but little research has been done on the numerical simulation of the factors affecting the thermal insulation performance of cold chain shipping containers. Therefore, this paper conducts the numerical simulation of the influencing factors to the thermal insulation performance of cold chain shipping container and studies the internal flow field. The structure and air supply diagrams of a cold chain shipping container were given, the thermal insulation performance of the thermal insulation sandwich panels in different surface layers and core layers of the cold chain shipping container was calculated and analyzed, and thermal inertia and heat transfer attenuation performance of the sandwich panels during the unsteady heat transfer process of the container were analyzed. The basic governing equations and assumptions were established for the internal flow field of the cold chain shipping container, and the distribution of the internal flow field was explored. With the impact of the viscosity of air molecules in the cold chain shipping container further ignored, the flow was regarded to be turbulent, and the internal flow field was simulated based on the turbulence-dissipation model. The experimental results were used to analyze the thermal insulation performance of cold chain shipping containers, and analysis results of the flow field where the cold chain shipping containers were stacked in different ways were given.

1. INTRODUCTION

In traditional shipping, the loss rate of aquatic products, meat, melons and fruits will be as high as 25%-30% in hot summer, resulting in a huge waste of resources [1-7]. To keep these goods fresh, cold chain shipping containers are used, where the air conditioning needs to keep the temperature inside at a very low level. A cold chain shipping container is somewhat similar to a refrigerator, but with a larger volume [8-17]. To prolong the shelf lives of products and reduce losses, according to traditional engineering experience, cold chain shipping containers containing food used during road, railway, and water transportation are often designed as cabinet models with uniform air temperature inside [18-22]. The existing control over the temperature inside a container body is actually the control over the temperature at the monitoring points, so it is necessary to numerically simulate the flow field and thermal insulation performance of cold chain shipping containers.

Shinoda et al. [23] regarded the roof shading of cold chain shipping containers as an energy-saving measure, and developed a general simulation method for predicting the surface temperatures of container walls based on computational fluid dynamics, which can be used as reference in this paper. This document investigated the feasibility of introducing roof shading on the basis of economic analysis. Through comparison with the experimental results at the Hakata port in Japan, it confirmed the effectiveness of the simulation method. Senguttuvan et al. [24] numerically analyzed the airflow pattern in a cold chain shipping container using several design models of the refrigeration unit, and proposed an improved refrigeration unit design to enhance the airflow distribution inside the cold chain shipping container. By changing the effective size and design parameters of the refrigeration unit, it considered 15 different models, which play important roles in the airflow patterns within a cold chain shipping container. In order to solve the inconvenient switching operation of the existing ventilation device and the loosening problem in the complex environment during transportation, Kaitai [25] designed a new type of container ventilation device, which adopted a rotary opening and an embedded sealing plug, and with the aid of a spring, effectively achieved stable and reliable opening and closing of the ventilation device. Due to its simple structure and convenient operation, this new type of ventilation device has broad application prospects in cold chain shipping containers.

In the simulation of the temperature or flow field of cold chain shipping containers, a lot of research results have been obtained from the cross-section temperature distribution, rather than from the simulation of the overall temperature or flow field distribution of cold chain shipping containers. To

optimize the thermal insulation performance of cold chain shipping containers, existing studies have attempted to change the thermal performance and thermal insulation mechanisms of the thermal insulation materials of the containers, but little research has been done on the numerical simulation of the factors affecting the thermal insulation performance of cold chain shipping containers. Therefore, this paper conducts the numerical simulation of the influencing factors to the thermal insulation performance of cold chain shipping container and studies the internal flow field. First, Section 2 shows the structure and air supply diagrams of a cold chain shipping container, calculates and analyzes the thermal insulation performance of the thermal insulation sandwich panels in different surface layers and core layers of the cold chain shipping container, and analyzes the thermal inertia and heat transfer attenuation performance of the sandwich panels during the unsteady heat transfer process of the container. Section 3 establishes the basic governing equations and assumptions for the internal flow field of the cold chain shipping container, and explores the distribution of the internal flow field. With the impact of the viscosity of air molecules in the cold chain shipping container further ignored, it regards the flow to be turbulent, and simulates the internal flow field based on the turbulence-dissipation model. Based on the experimental results, this section analyzes the thermal insulation performance of cold chain shipping containers, and gives the analysis results of the flow field where the cold chain shipping containers were stacked in different ways.

2. ANALYSIS OF THERMAL INSULATION PERFORMANCE OF COLD CHAIN SHIPPING CONTAINERS

A cold chain shipping container is of a galvanized steel structure, where the inner walls, bottom plate, top plate and door are made of metal clad plates, aluminum plates, stainless steel plates or polyester. Container size and performance have been standardized internationally. The operating temperature range is -30°C~12°C, and the more general range is -30~20°C. Due to the good thermal conductivity of steel, the thermal insulation performance of cold chain shipping containers is poor in winter and summer. This paper firstly calculates and analyzes the thermal insulation performance of the thermal insulation sandwich panels in different surface layers and core layers of a cold chain shipping container, and analyzes the thermal inertia and heat transfer attenuation performance of the sandwich panels during the unsteady heat transfer process of the container. Figure 1 and Figure 2 show the structure of a cold chain shipping container and how air supply is achieved, respectively.

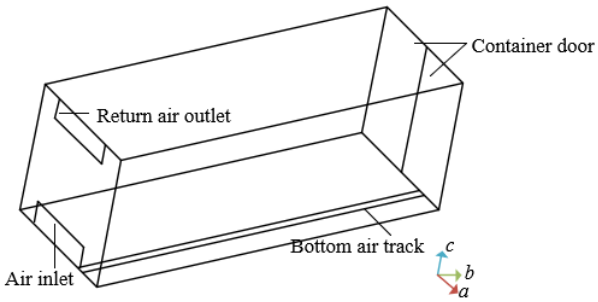

Figure 1. Structure of a cold chain shipping container

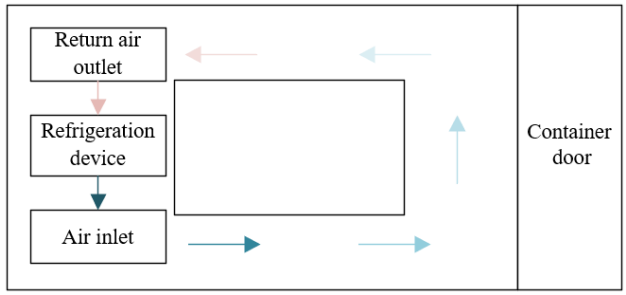

Figure 2. Air supply of a cold chain shipping container

In this paper, the relatively simple and easy-to-use harmonic analysis method was used to calculate the thermal stability indicators of the thermal insulation sandwich panel structure of the cold chain shipping container, as it can more directly compare the thermal insulation performance of the thermal insulation material under different sandwich panel structures.

In actual engineering, the thermal insulation sandwich panel structure of a cold chain shipping container has some flat walls with a limited thickness, which causes one or both sides of the container to be subjected to thermal action with periodic fluctuations. In order to solve the above-mentioned heat transfer problem of container insulation materials, this section divided and calculated the time periods of the complex heat transfer process, and then superimposed the time periods to obtain the final calculation result.

Eq. (1) and (2) express the harmonic heating effects on both sides of the flat wall of a cold chain shipping container under the action of the inner and outer two-way simple harmonic waves. Assuming that the temperature of the outer sandwich panel medium is represented by ψ_o, that the average temperature of the outer sandwich panel medium in one period by ψ'_o, that the amplitude of the temperature wave of the outer sandwich panel medium by X_o, that the initial phase of the temperature wave of the outer sandwich panel medium by Ψ_o, that the period of the temperature wave by C, and that the computation time by τ, then there is:

$$\Psi_o = \Psi'_o + X_o cos\left(\frac{2\pi\tau}{C} - \Psi_o\right) \tag{1}$$

Assuming that the temperature of the inner sandwich panel medium is represented by ψ_i, that the average temperature of the inner sandwich panel medium in a period by ψ'_i, that the amplitude of the temperature wave of the outer sandwich panel by X_i, and that the initial phase of the temperature wave of the outer sandwich panel medium by Ψ_i, then there is:

$$\psi_i = \psi'_i + X_i \cos\left(\frac{2\pi\tau}{C} - \Psi_i\right) \tag{2}$$

The complex heat transfer process can be decomposed into the following three sub-processes:

One of the sub-processes is the stable heat transfer under ψ'_i and ψ'_o. Assuming that the heat transfer coefficient of the inner surface of the thermal insulation sandwich panel in the cold chain shipping container is represented by S_i, and that the heat flow through the sandwich panel structure per unit time by S_0, then the average temperature of the inner surface of the thermal insulation sandwich panel under this condition can be calculated by Eq. (3):

$$\omega_i' = \psi_i' - \frac{S_i}{S_0}\left(\psi_i' - \psi_e'\right) \tag{3}$$

The second sub-process is the periodic unsteady heat transfer on the outside of the thermal insulation sandwich panel in the cold chain shipping container under the action of thermal harmonics alone. Assuming that the amplitude and initial phase of the inner surface temperature wave of the sandwich panel structure under this condition are represented by $X_{ig.o}$, and $\Psi_{ig,o}$, the corresponding inner surface temperature of the sandwich panel structure can be calculated by Eq. (4):

$$\omega_{ig,o} = X_{ig,o} \cdot cos\left(\frac{2\pi\tau}{C} - \Psi_{ig,o}\right) \tag{4}$$

Assuming that the amplitude attenuation factor of the thermal harmonics from outside to the inner surface of the sandwich panel structure through the thermal insulation material is represented by $\alpha_{o,ig}$, and that the corresponding delay time by $\Psi_{o,ig}$, there is:

$$X_{ig,o} = \frac{X_o}{\alpha_{o-i\tau}}, \Psi_{ig,o} = \Psi_o + \Psi_{o-ig} \tag{5}$$

The third sub-process is the periodic unsteady heat transfer inside the thermal insulation sandwich panel structure of the cold chain shipping container under the action of thermal harmonics alone. Under this condition, supposing that the amplitude and initial phase of the inner surface temperature wave of the sandwich panel structure are represented by $X_{ig.i}$ and $\Psi_{ig,i}$, the corresponding inner surface temperature of the sandwich panel structure can be calculated by Eq. (6):

$$\omega_{ig,i} = X_{ig,i} \cdot cos\left(\frac{2\pi\tau}{C} - \Psi_{ig,i}\right) \tag{6}$$

Assuming that the amplitude attenuation factor of the inner thermal harmonics to the inner surface of the sandwich panel structure through the thermal insulation material is represented by $\alpha_{i,ig}$, and that the corresponding phase delay is represented by $\Psi_{i,ig}$, there is:

$$X_{ig,i} = \frac{X_o}{\alpha_{i-i\tau}}, \Psi_{ig,i} = \Psi_i + \Psi_{i-ig} \tag{7}$$

Based on the above analysis, the following formula shows how to calculate the inner surface temperature of the thermal insulation sandwich panel structure of the cold chain shipping container under the action of two-way harmonics:

$$\begin{aligned}\omega_i' &= \psi_i' - \frac{S_i}{S_0}\left(\psi_i' - \psi_o'\right) + \\ &\frac{X_o}{\alpha_{o-i\tau}} cos\left[\frac{2\pi\tau}{C} - \left(\Psi_o - \Psi_{o-ig}\right)\right] \\ &+ \frac{X_o}{\alpha_{i-i\tau}} cos\left[\frac{2\pi\tau}{C} - \left(\Psi_i + \Psi_{i-ig}\right)\right]\end{aligned} \tag{8}$$

This paper only considers the changes in the inner surface temperature of the thermal insulation sandwich panel under the action of the harmonics of the air temperature outside the cold chain shipping container. Under this condition, the inner surface temperature of the thermal insulation sandwich panel can be simplified as follows:

$$\overline{\omega_i} = \frac{S_i}{S_0}\overline{\psi_e} + \frac{X_o}{\alpha_{o-i\tau}} \cos\left[\frac{2\pi\tau}{C} - \left(\Psi_o + \Psi_{o-ig}\right)\right] \tag{9}$$

It can be seen from the above analysis that S_0 is closely related to $\alpha_{o,ig}$, and $\Psi_{o,ig}$, so the harmonics of the inner surface temperature of the thermal insulation sandwich panel structure can be obtained based on the calculation of $\alpha_{o,ig}$, and $\Psi_{o,ig}$.

The calculation of the harmonic amplitude attenuation factor and phase delay is complicated. In order to obtain accurate calculation results, an approximate calculation method was introduced in this paper. Assuming that the heat storage coefficient of each layer of the sandwich panel from the inside to the outside is represented by R_1, R_2..., R_m, that the heat storage coefficient of the outer surface of each layer in the sandwich panel from the inside to the outside by $B_{1,o}$, $B_{2,o}$..., $B_{m,o}$, that the heat transfer coefficients of the inner and outer surfaces of the sandwich panel by β_i and β_o, respectively, and that the attenuation factor of the sandwich panel structure by $\alpha_{o,ig}$, the following formula shows how to calculate the attenuation factor of the temperature harmonics transmitted from outside the thermal insulation sandwich panel to its inner surface:

$$\begin{aligned}\alpha_{o-ig} = 0.9o^{\frac{\sum C}{\sqrt{2}}} &\frac{R_1 + \beta_i}{R_1 + B_{1,o}} \cdot \frac{R_2 + B_{1,o}}{R_2 + B_{2,o}} \cdot \\ \cdots &\frac{R_m + B_{m-1,o}}{R_m + B_{m,o}} \cdot \frac{B_{m,o} + \beta_o}{\beta_o}\end{aligned} \tag{10}$$

The following formula shows how to calculate the phase delay of the temperature harmonics from outside the sandwich panel to its inner surface:

$$\begin{aligned}\Psi_{o-ig} &= 40.5\sum C + arctan\frac{B_{og}}{B_{og} + \beta_o\sqrt{2}} \\ &-arctan\frac{\beta_i}{\beta_i + B_{ig}\sqrt{2}}\end{aligned} \tag{11}$$

Assuming that the heat storage coefficient of the outer surface of the thermal insulation sandwich panel in the cold chain shipping container is represented by B_{og}, and that the heat storage coefficient of the inner surface by $B_{i\,g}$, substitute $\Psi_{o,ig}$ for $\Psi_{i,ig}$, then, $\delta_{o,ig}=c/2\pi\tau\Psi_{o,ig}$, and the delay time of the outer temperature of the container transmitted to the inner surface of the sandwich panel through the thermal insulation material is calculated as follows:

$$\delta_{o-ig} = \frac{1}{15}\left(\begin{aligned}&40.5\sum C + arctan\frac{B_{og}}{B_{og} + \beta_o\sqrt{2}} \\ &-arctan\frac{\beta_i}{\beta_i + B_{ig}\sqrt{2}}\end{aligned}\right) \tag{12}$$

If the thermal inertia index C of a certain layer l is greater than 1, there is:

$$B_{l,o} = R_l \tag{13}$$

If the thermal inertia index C of a certain layer l is less than 1, there is:

$$B_{l,o} = \frac{S_l R_l^2 + B_{l-1,o}}{1 + S_l B_{l-1,o}} \tag{14}$$

If the thermal inertia index C of the first layer is less than 1, there is:

$$B_{l,o} = \frac{S_1 R_1^2 + \beta_i}{1 + S_1 \beta_i} \tag{15}$$

If the thermal insulation adopts the multi-layer sandwich panel structure, the heat storage coefficient of the outer surface should be equivalent to that of the outer surface of the last thermal insulation layer. Then there is:

$$B_{og} = B_{m,o} \tag{16}$$

For the calculation of the heat storage coefficient of the inner surface, the heat storage coefficient $B_{l,\,i}$ of the inner surface of the l-th layer that is closest to the inner surface and for which, C is greater than 1, is considered as R_l, and then perform the calculation layer by layer from this layer until $B_{1,i}$.

Assuming that the thermal resistance value of the i-th layer of the sandwich panel is represented by S_i, that the thermal resistance value of the i-th layer by R_i, that the corresponding thickness by c_i, and that the corresponding thermal conductivity by μ_i, the following formula shows how to calculate the thermal inertia index C of the sandwich panel:

$$C = \sum_{i=1}^{m} S_i R_i = R_1 \frac{c_1}{\mu_1} + R_2 \frac{c_2}{\mu_2} + \ldots + R_m \frac{c_m}{\mu_m} \tag{17}$$

3. ANALYSIS OF THE INTERNAL FLOW FIELD OF COLD CHAIN SHIPPING CONTAINERS

In order to explore the distribution of the flow field inside the cold chain shipping container, the basic governing equations and assumptions were established in this paper. Since the impact of the viscosity of air molecules in the cold chain shipping container is ignored, and its flow is regarded as to be turbulent, the turbulence-dissipation model was used to simulate the internal flow field. Assuming that the turbulent pulsation kinetic energy in the cold chain shipping container is represented by l, and that the dissipation rate of l by σ, the corresponding turbulent pulsation kinetic energy equation is given by Eq. (18):

$$\begin{aligned} &\phi \frac{\partial l}{\partial \tau} + \phi v_j \frac{\partial l}{\partial aj} = \frac{\partial}{\partial a_j}\left[\left(\lambda + \frac{\lambda_p}{\varepsilon_l}\right)\frac{\partial l}{\partial aj}\right] \\ &+ v_\tau \frac{\partial v_i}{\partial a_j}\left(\frac{\partial v_i}{\partial a_j} + \frac{\partial v_j}{\partial a_i}\right) - \phi\sigma \end{aligned} \tag{18}$$

The corresponding dissipation rate equation is given as follows:

$$\begin{aligned} &\phi \frac{\partial \sigma}{\partial \tau} + \phi v_l \frac{\partial \sigma}{\partial a_l} = \frac{\partial}{\partial a_l}\left[\left(\lambda + \frac{\lambda_\tau}{\varepsilon_\sigma}\right)\frac{\partial l}{\partial a_l}\right] \\ &+ \frac{d_1 \sigma}{l} v_\tau \frac{\partial v_i}{\partial a_j}\left(\frac{\partial v_i}{\partial a_j} + \frac{\partial v_j}{\partial a_i}\right) - d_2 \phi\sigma \end{aligned} \tag{19}$$

Assuming that the air density is represented by φ, that the air velocity vector by U, which satisfies $U=((v, u, q)^T$, and the dependent variable by ρ, which satisfies $\rho=\{1, v, u, q, \sigma\}$, that the diffusion coefficient corresponding to ρ by R_ρ and that the source term by χ_ρ, the overall governing equations for heat transfer and air flow established in a cold chain shipping container are given as follows:

$$\frac{\partial(\varphi\rho)}{\partial p} + div(\varphi U\rho) = div(\chi_\rho grad\rho) + R_\rho \tag{20}$$

$$\lambda_p = SH_\lambda \varphi l^2 / \sigma \tag{21}$$

In order to explore the changes in the flow field of the cold chain shipping container under the influences of different supply air speeds, the turbulence intensity, flow scale, hydraulic diameter and other turbulence parameters under different supply air speeds were set. Assuming that the Reynolds number is represented by LN, that the density of the fluid by κ, that the dynamic viscosity coefficient of the sandwich panel medium by γ, and that the average velocity by U, the following formula gives the definition formula of the turbulence intensity TU:

$$TU = 0.16(LN_{DH})^{-0.125} \tag{22}$$

$$LN_{DH} = \frac{Ud\kappa}{\gamma} \tag{23}$$

Assuming that the width and length of a non-circular tube with a square flow shape are represented by x and y, that the hydraulic diameter is equivalent to 4 times the corresponding cross-sectional area, represented by k, and that the wetted perimeter factor is 0.07, the characteristic scale of the turbulence CS is calculated according to Eq. (24) and (25):

$$k = 0.07CS \tag{24}$$

$$CS = \frac{2(xy)}{x + y} \tag{25}$$

Assuming that the average velocity is denoted by U, and that the turbulent kinetic energy l is estimated based on TU, there is:

$$l = \frac{3}{2} \times (U \cdot CS)^2 \tag{26}$$

Assuming that the empirical constant is represented by EM_λ,

and that the turbulent dissipation rate σ is estimated by further using l and TU, then there is:

$$\sigma = EM_{\lambda}^{\frac{3}{4}} \frac{l^{\frac{3}{2}}}{CS} \tag{27}$$

4. EXPERIMENTAL RESULTS AND ANALYSIS

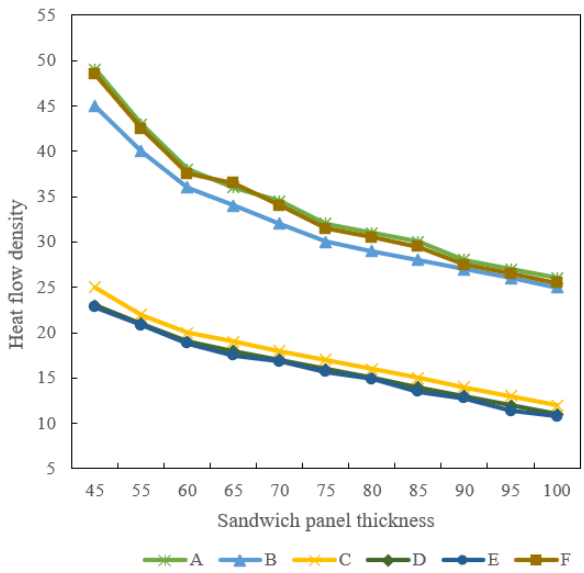

Figure 3. Heat flow density diagram of the sandwich panel in a cold chain shipping container

The thermal insulation performance of the cold chain shipping container was first analyzed. Figure 3 shows the heat flow density diagram of the sandwich panel in the cold chain shipping container. It can be seen that with the increase of the thickness of the thermal insulation sandwich panel, the heat flow density gradually decreased. Through comparison, no significant difference was found in the flow density of the sandwich panels in the calcium silicate board, steel plate and thin slab layers, nor is any significant difference found in the flow density of the sandwich panels in the insulation coating, aerogel and foam board layers.

With the surface layer thickness of the thermal insulation ranging between 0.5~1mm, and the thickness of the sandwich panel between 50-200mm, the thermal insulation performance indices of the cold chain shipping container were analyzed and calculated. The specific indices include the thermal inertia, attenuation factor, and delay time. Table 1 shows the thermal insulation performance indices of different combinations of sandwich panel thicknesses.

It can be seen from the table that, for the thermal insulation sandwich panel, since the steel surface layer is thin and has good thermal conductivity, the effect of the surface layer thickness on the thermal inertia index of the thermal insulation sandwich panel can be ignored. Increasing the core thickness of the thermal insulation sandwich panel or selecting a core material with better thermal insulation performance is an important way to improve its thermal inertia. For the thermal insulation using the same core material, as the thickness of the surface layer increases, the attenuation factor of the thermal harmonics passing through the sandwich panel will gradually increase, and the temperature change inside the container will gradually decrease under the impact of the temperature fluctuations outside the container. The thermal insulation with a thicker sandwich panel can obtain a larger attenuation factor. At the same time, for the thermal insulation using the same core material, as the thickness of the surface layer increases, the delay time of the thermal harmonics passing through the sandwich panel will also increase gradually. For sandwich panels with the same surface layers but different core layers, the delay time will vary greatly.

Figure 4 shows the curve of temperature change inside the cold chain shipping container under different feature lines and stacking methods, and Figure 5 shows the curve of air speed change of the cold chain shipping container under different feature lines and stacking methods. 6 goods stacking methods were compared, namely empty container, integral type, horizontal two-piece, vertical two-piece, layered two-piece, and four-piece stacking, corresponding to (1), (2), (3), (4), (5) and (6), and the feature lines for data collection included the connecting lines between the center points on the front and rear sides and on the left and right sides of the container.

Table 1. Thermal insulation performance indices of different combinations of sandwich panel thicknesses

Parameter index	Sandwich panel thickness	Surface layer thickness					
		0.5	0.6	0.7	0.8	0.9	1
Thermal inertia index	50	0.7481	0.7064	0.7152	0.7596	0.7158	0.7518
	100	1.6259	1.0251	1.2629	1.2414	1.9269	1.3291
	150	2.3052	2.3069	2.3014	2.3062	2.3514	2.5147
	200	2.6924	2.5184	2.6582	2.4185	2.6258	2.3968
Attenuation factor	50	2.3052	2.1471	2.5182	2.0514	2.4585	2.0514
	100	4.6247	4.6253	4.3269	4.4274	4.6239	5.1429
	150	6.2051	7.5182	7.2514	7.6258	7.2513	8.3251
	200	13.2047	13.6295	16.3258	10.2051	14.2409	15.2631
Delay time	50	1.8362	1.8174	2.0517	2.3069	2.1038	1.1471
	100	3.6259	3.2518	3.6324	3.1271	3.2513	2.6248
	150	5.4524	5.3629	5.0125	4.6329	6.2118	5.3056
	200	6.9052	7.2847	7.2036	7.2513	7.6235	7.2958

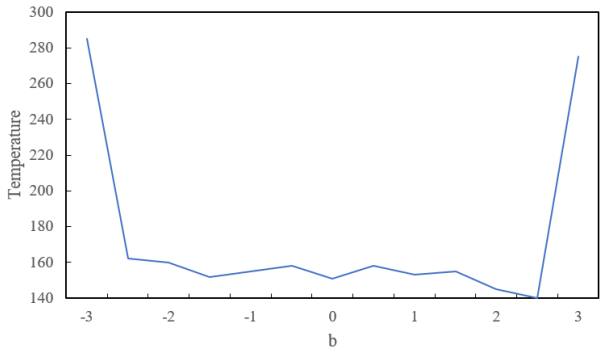

1)

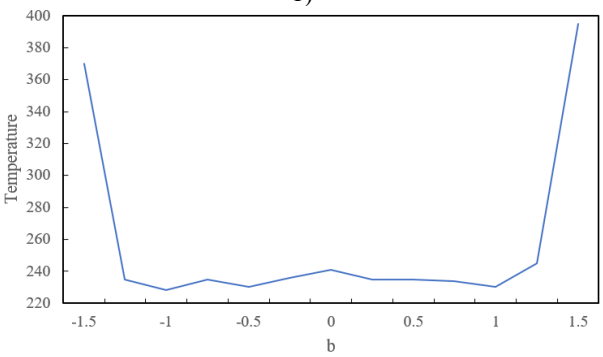

2)

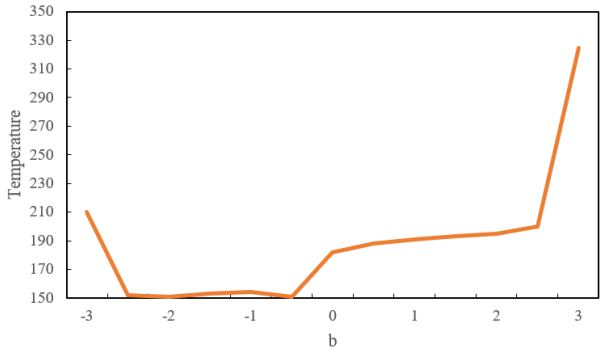

3)

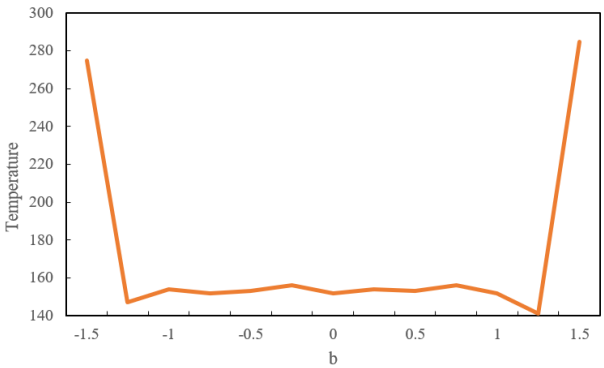

4)

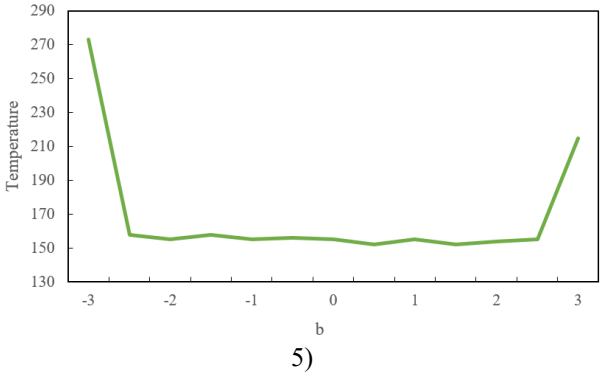

5)

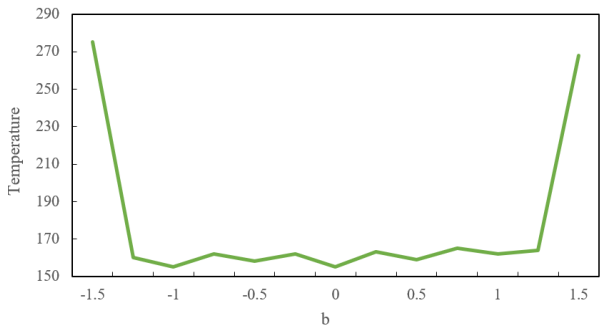

6)

Figure 4. Curve of temperature change inside the cold chain shipping container under different stacking methods

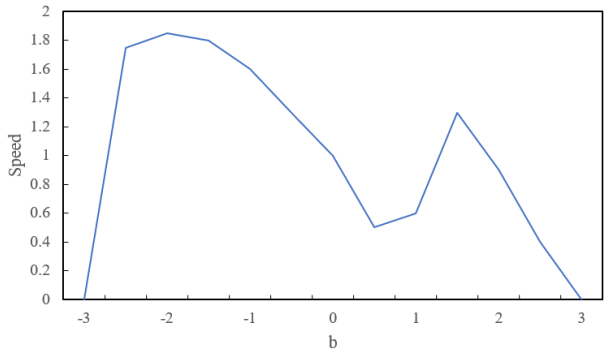

1)

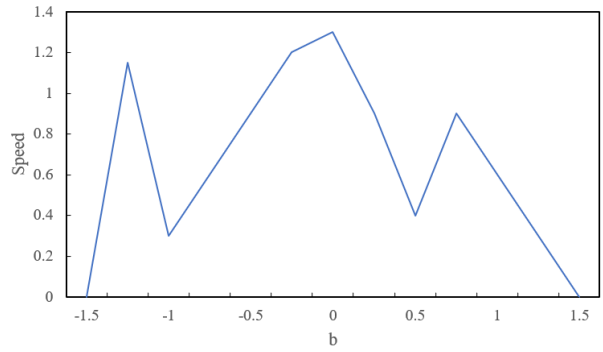

2)

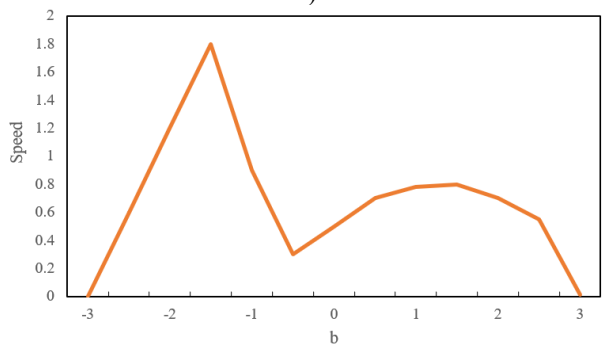

3)

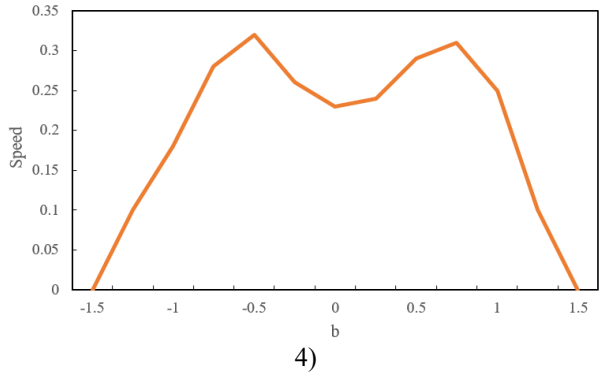

4)

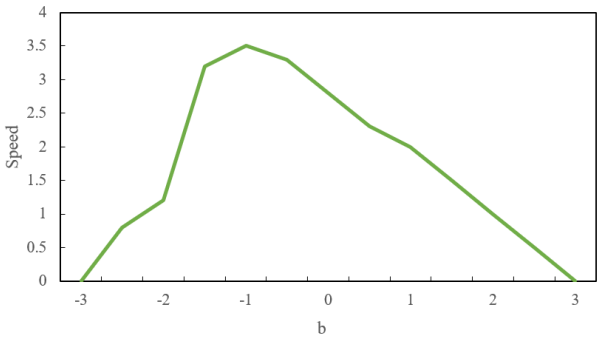

5)

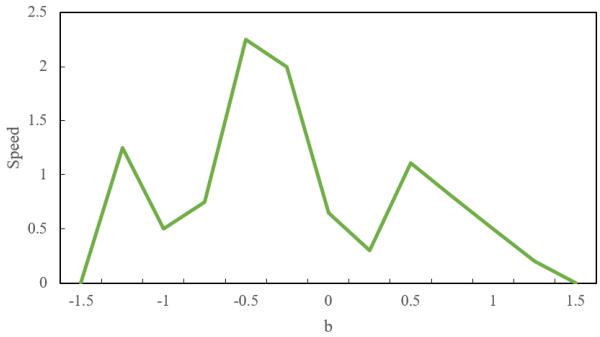

6)

Figure 5. Curve of air speed change in the cold chain shipping container under different stacking methods

From analysis of Figures 4 and 5, it can be seen that when the cold chain shipping container was empty, the cold air refrigerated could be transported to various positions in the container space, and the eddy current and slow refrigeration caused by the unbalanced cold air flow did not occur under this stacking method, and the temperature distribution on the boundaries and the feature lines is uniform, indicating that the temperature and speed of the cold air at this time are proper. When the goods were stacked by the integral-type or two-piece method in the cold chain shipping container, the area around the top of the container door was prone to accumulation of high-temperature air, and the upper layer of the goods generated eddy currents that caused high-temperature air to accumulate. Therefore, in a cold chain shipping container, goods cannot be stacked too high, it must not be stacked too high, and there should be enough clearance between the upper layer of goods and the top of the container for cold air circulation. Judging from the uniformity of the cold air circulation distribution, the integral-type stacking method had the worst performance, followed by the layered two-piece method, and the horizontal and vertical two-piece methods had slightly better performance. None of the 4 goods stacking methods achieved the desired refrigeration and air circulation effects, and all caused a certain waste of cooling capacity. When the goods were stacked by the four-piece method in the cold chain shipping container, the two vertical and horizontal passages reserved for ventilation helped take away the high-temperature air in the goods through the supply air-return air circulation in time, and effectively increased the circulation efficiency of cold air inside the container. Compared with that under the integral-type or two-piece stacking method, the refrigerated cold air reached various positions of the cold chain shipping container in a more uniform and effective way, leading to better cold air circulation and better refrigeration effect.

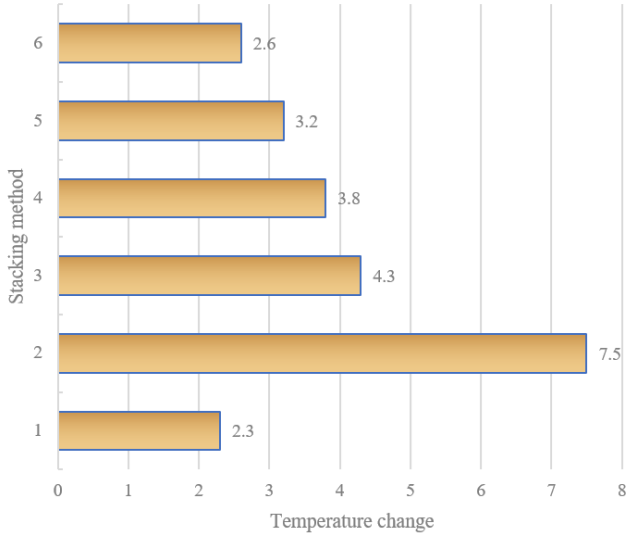

Figure 6. Comparison of temperature differences in the cold chain shipping container under different stacking methods

Figure 6 compares the temperature differences in a cold chain shipping container under different stacking methods. It can be seen that the largest temperature difference appeared in the container with the integral-type stacking method, while the smallest difference in the empty container and the one with the four-piece stacking method. This shows that the stacking method with cold air channels produces smaller eddy current of air and better cooling effects. Among the three types of stacking methods, namely horizontal two-piece, vertical two-piece, and layered two-piece methods, the vertical two-piece method achieved the smallest temperature difference in the container, where the flow field distribution was the most uniform, and the utilization rate of the container capacity reached the maximum. The four-piece stacking method reserved one vertical passage and one horizontal one for ventilation, which effectively improved the heat convection and heat exchange between the cold air and the goods. The high-temperature air in the container could be taken out in time through the supply air-return air circulation, making the distribution of the flow field relatively uniform. Therefore, the four-piece stacking method is the desired stacking method for cold chain shipping containers.

5. CONCLUSIONS

This paper conducts the numerical simulation of the influencing factors to the thermal insulation performance of cold chain shipping container and studies the internal flow field. The structure and air supply diagrams of a cold chain shipping container were given, the thermal insulation performance of the thermal insulation sandwich panels in different surface layers and core layers of the cold chain shipping container was calculated and analyzed, and thermal inertia and heat transfer attenuation performance of the sandwich panels during the unsteady heat transfer process of the container were analyzed. The basic governing equations and assumptions were established for the internal flow field of the cold chain shipping container, and the distribution of the internal flow field was explored. With the impact of the viscosity of air molecules in the cold chain shipping container further ignored, the flow was regarded to be turbulent, and the

internal flow field was simulated based on the turbulence-dissipation model.

The experimental results provided the heat flow density diagram of the sandwich panel in the cold chain shipping container. It can be seen that with the increase of the thickness of the thermal insulation sandwich panel, the heat flow density gradually decreased. The thermal insulation performance indices of different combinations of sandwich panel thicknesses were summarized. The temperature change curves and air speed change curves in the cold chain shipping container under different feature lines and stacking methods were drawn. The performance of 6 goods stacking methods, namely empty container, integral type, horizontal two-piece, vertical two-piece, layered two-piece and four-piece methods, were analyzed, and the temperature differences in the cold chain shipping containers under different stacking methods were compared, which led to the conclusion that the four-piece stacking method is a desired method for cold chain shipping containers.

REFERENCES

[1] Miao, H. (2022). Cold chain logistics route optimization based on ant colony algorithm. In The International Conference on Cyber Security Intelligence and Analytics, 983-989. https://doi.org/10.1007/978-3-030-97874-7_143

[2] Wang, S. (2022). Study on cold chain logistics operation and risk control of fresh e-commerce products. Advances in Multimedia, 2022: Article ID 7272370. https://doi.org/10.1155/2022/7272370

[3] Li, K., Li, D., Wu, D. (2022). Carbon transaction-based location-routing-inventory optimization for cold chain logistics. Alexandria Engineering Journal, 61(10): 7979-7986. https://doi.org/10.1016/j.aej.2022.01.062

[4] Ren, Q.S., Fang, K., Yang, X.T., Han, J.W. (2022). Ensuring the quality of meat in cold chain logistics: A comprehensive review. Trends in Food Science & Technology, 119: 133-151. https://doi.org/10.1016/j.tifs.2021.12.006

[5] Chen, Q., Qian, J., Yang, H., Wu, W. (2022). Sustainable food cold chain logistics: From microenvironmental monitoring to global impact. Comprehensive Reviews in Food Science and Food Safety, 21(5): 4189-4209. https://doi.org/10.1111/1541-4337.13014

[6] Tao, S., Wang, F., Wei, Q. (2022). Research on multi-objective cold chain logistics distribution path optimization based on fuzzy time window constraints. Conference Proceedings of the 10th International Symposium on Project Management, China, ISPM 2022, pp. 970-976.

[7] Wang, Z., Wang, X., Guo, J. (2022). Research on collaborative optimization of pharmaceutical cold chain logistics inventory and distribution. In Proceedings of the Asia Conference on Electrical, Power and Computer Engineering, pp. 1-6. https://doi.org/10.1145/3529299.3530205

[8] Nordtvedt, T.S., Widell, K.N. (2020). Refrigeration and sustainability in the seafood cold chain. In Refrigeration Science and Technology, 13-24. https://doi.org/10.18462/iir.iccc.2020.314814

[9] Han, Z., Hua, L., Fang, Y., Ma, Q., Li, Y., Wang, J.X. (2020). Innovative research on refrigeration technology of cold chain logistics. In IOP Conference Series: Earth and Environmental Science, 474(5): 052105. https://doi.org/10.1088/1755-1315/474/5/052105

[10] Kammuang-lue, N., Pattana, S., Tachajapong, W., Wiratkasem, K. (2022). Preliminary evaluation on specific energy consumption of refrigerated trucks in Thailand's cold chain used for national energy policy planning. Energy Reports, 8(S9): 1314-1320. https://doi.org/10.1016/j.egyr.2022.07.093

[11] González-Vidal, A., Gómez-Bernal, P., Mendoza-Bernal, J., Skarmeta, A.F. (2021). BIGcoldTRUCKS: a BIG data dashboard for the management of COLD chain logistics in refrigerated TRUCKS. In 2021 IEEE International Conference on Big Data (Big Data), pp. 2894-2900. https://doi.org/10.1109/BigData52589.2021.9671633

[12] Gao, E., Cui, Q., Jing, H., Zhang, Z., Zhang, X. (2021). A review of application status and replacement progress of refrigerants in the Chinese cold chain industry. International Journal of Refrigeration, 128: 104-117. https://doi.org/10.1016/j.ijrefrig.2021.03.025

[13] Kagawa, N. (2020). New refrigerants and sustainable refrigerant management for cold chain -Current situation in Japan and future aspect. Refrigeration Science and Technology, 6th IIR Conference on Sustainability and the Cold Chain, pp. 211-218.

[14] Alvarez, G. (2015). Cold chain refrigeration innovations the FRISBEE project. Journal of Food Engineering, 148: 1-1. https://doi.org/10.1016/j.jfoodeng.2014.11.010

[15] Pérez, E.V., Ortega, O.B., Villa, J.L. (2019). IoT circuit design to monitor cold chain refrigerators. In 2019 Latin American Electron Devices Conference (LAEDC), 1: 1-5. https://doi.org/10.1109/LAED.2019.8714747

[16] Meneghetti, A., Dal Magro, F., Simeoni, P. (2018). Fostering renewables into the cold chain: How photovoltaics affect design and performance of refrigerated automated warehouses. Energies, 11(5): 1029. https://doi.org/10.3390/en11051029

[17] Vailati Riboni, F., Comazzi, B., Castelnuovo, G., Molinari, E., Pagnini, F. (2018). Lecture notes of the institute for computer sciences, social-informatics and telecommunications engineering, LNICST. Cloud Infrastructures, Services, and IoT Systems for Smart Cities - 2nd EAI International Conference, 189: 76-83. https://dx.doi.org/10.1007/978-3-030-01093-5_15

[18] Amat, S., Legaz, M. J., Morilla, E. (2018). Modeling the refrigeration system of a maritime container. Maritime Transportation and Harvesting of Sea Resources, 2: 973-979.

[19] Kim, H., Jeong, H., Park, T. (2019). Distribution scheduling model of multiple temperature refrigerated container system. In Proceedings of the 2019 5th International Conference on E-Business and Applications, pp. 105-109. https://doi.org/10.1145/3317614.3317628

[20] Sørensen, K.K., Skovrup, M.J., Jessen, L.M., Stoustrup, J. (2015). Modular modeling of a refrigeration container. International Journal of Refrigeration, 55: 17-29. https://doi.org/10.1016/j.ijrefrig.2015.03.017

[21] Getahun, S., Ambaw, A., Delele, M., Meyer, C.J., Opara, U.L. (2017). Analysis of airflow and heat transfer inside fruit packed refrigerated shipping container: Part I-Model development and validation. Journal of Food Engineering, 203: 58-68. https://doi.org/10.1016/j.jfoodeng.2017.02.010

[22] Zhang, M., Sun, J., Fricke, B., Nawaz, K., Gluesenkamp, K., Shen, B., Liu, X. (2022). A study on computational fluid dynamics modeling of a refrigerated container for COVID-19 vaccine distribution with experimental validation. International Communications in Heat and Mass Transfer, 130: 105749. https://doi.org/10.1016/j.icheatmasstransfer.2021.105749

[23] Shinoda, T., Budiyanto, M.A., Sugimura, Y. (2022). Analysis of energy conservation by roof shade installations in refrigerated container areas. Journal of Cleaner Production, 377: 134402. https://doi.org/10.1016/j.jclepro.2022.134402

[24] Senguttuvan, S., Youn, J.S., Park, J., Lee, J., Kim, S.M. (2020). Enhanced airflow in a refrigerated container by improving the refrigeration unit design. International Journal of Refrigeration, 120: 460-473. https://doi.org/10.1016/j.ijrefrig.2020.08.019

[25] Kaitai, H. (2019). Study on a new type of air-exchange device for refrigerated container. In IOP Conference Series: Earth and Environmental Science, 332(3): 032054. https://doi.org/10.1088/1755-1315/332/3/032054